RSC Advances

PAPER

View Article Online
View Journal | View Issue

Computational insight of the mechanism of Algar–Flynn–Oyamada (AFO) reaction†

Cite this: *RSC Adv.*, 2014, **4**, 18702

Shubhankar Bhattacharyya*[a] and Kaushik Hatua*[b]

Received 12th November 2013
Accepted 26th March 2014

DOI: 10.1039/c3ra46623j

www.rsc.org/advances

The present DFT investigation supports a previous conclusion of Dean *et al.* that hydroxylation occurs without epoxide intermediate at room temperature due to a strong electrostatic interaction of peroxide ions with π electrons of C=C bonds of chalcone, and 3-hydroxyflavone has been found to be the major product. The calculated activation energy difference ($\Delta G^{\#}$) of initial enolization followed by hydroxylation or simultaneous cyclization and hydroxylation has been found to be negligible (~4 kcal mol^{-1}). On the other hand, epoxide formation requires significant activation energy, which is supposed to occur at high temperatures. In addition, if epoxide is formed, the ring opens by an attack of phenolic oxygen, occurring preferentially at α position *via* a five-member transition state due to a low activation barrier height (19.82 kcal mol^{-1} in the gas phase and 19.55 kcal mol^{-1} in ethanol) compared to that of a six-member transition state (44.41 kcal mol^{-1} at B3LYP in the gas phase and 38.55 kcal mol^{-1} in ethanol). It is also observed that the solvation study does not affect the main conclusion of the paper. These findings also support the previous observation of Dean *et al.* Predicted $\Delta G^{\#}$ in different DFT functionals are consistent, although the total energy is significantly different.

Introduction

3-Hydroxyflavones are the most versatile naturally occurring plant pigments.[1] These compounds are often found in fruits (particularly in skin), vegetables, and plant tissues.[2] Thus, it is a common component in the general daily diet of human beings. In the human body, these compounds exhibit various pharmacological properties, which include antioxidant,[3a] anti-allergenic,[3b] antimicrobial,[3c] antifungal,[3d] antiviral,[3e] and anticancer properties.[3f–3h] These classes of molecules are the secondary metabolites of plants,[4] having the basic skeletal structure of the 2-phenyl benzopyranone moiety. The structure of the 2-phenyl benzopyranone skeleton plays a crucial role in imparting antioxidant and other pharmacological properties.[5] The implementation of several functional groups to this 2-phenyl benzopyranone skeleton can influence overall biological properties. By applying suitable functional group manipulation, flavonoids exhibit significant biological activities and can be used in medicines. Because of their undeniable biological as well as medical importance, they have attracted remarkable attention to the pharmacological and nutritional fields.[6] During the past century, various methods had been reported the chemical synthesis of 3-hydroxyflavones from different sources.[7] However, over time, the Algar–Flynn–Oyamada (AFO) reaction[8] has proven to be most versatile and straightforward method to access 3-hydroxyflavones from chalcones in the presence of alkaline hydrogen peroxide at room temperature. Currently, this reaction has become of great importance, both industrially and pharmaceutically. After the discovery of the Algar–Flynn–Oyamada reaction, many experimental efforts were carried out to elucidate the mechanism of reaction. In addition, attempts were undertaken to identify intermediates and the overall course of the reactions, and numerous possible reaction pathways have been proposed. Currently, the emphasis has focused on improving this reaction to develop a simple, facile, and convenient synthetic procedure for the preparation of 3-hydroxylflavone from chalcones. Thus, it is necessary to thoroughly understand the total course of the reaction. In addition, to obtain improved efficiency and elegancy of the reaction, profound knowledge of the reaction mechanism at the molecular level is highly essential. In this regard, computational chemistry techniques have demonstrated to be an adequate complementary tool for explaining, guiding, and predicting synthetic organic chemistry experiments on the basis of a theoretically predicted reaction mechanism. To the best of our knowledge, no such efforts have been made to understand theoretical and mechanistic insights of the reaction.

Initially, it was assumed[9] that the reaction was induced *via* a key intermediate, an epoxide that further ring opening through β-attack leads to 3-hydroxyflavanone (path-1). In addition, a

[a]*Synthetic Chemistry Division, Defense R & D Establishment, Jhansi Road, Gwalior 474002, India. E-mail: shubhankar_chem@yahoo.co.in*

[b]*Department of Chemistry, Bengal Engineering & Science University, Shibpur-711103, India. E-mail: kaushikhatua@gmail.com*

† Electronic supplementary information (ESI) available: Gas phase optimized equilibrium geometry at B3LYP/6-31+G(d,p) of all the reactants, intermediates, and transition states with selected bond length (Å) and cartesian coordinates have been given in the supporting information. See DOI: 10.1039/c3ra46623j

consequence of further 3-hydroxyflavanone oxidation yielded the final product of 3-hydroxyflavone. Later, Dean and Podimuang[10] proposed that the AFO reaction, the formation of 3-hydroxyflavone from 2′-hydroxychalcone occurred *via* a combination of cyclization and oxidation rather than through an epoxide intermediate. According to Dean and Podimuang, the epoxidation of 2′-hydroxychalcone requires an attack at the β-position of chalcone by hydroperoxide anion, which would be highly difficult in the case of 2′-hydroxychalcones (phenolic chalcones). 2′-Hydroxychalcone is converted into anions under this strongly alkaline reaction condition, and the delocalization of the negative charge leads to columbic repulsion of the hydroperoxide anion, resulting in internal electronic inactivation of the reaction. O'Sullivan[11] has shown that the AFO reaction involves the alkaline hydrogen peroxide oxidation of the 2′-hydroxychalcones, first into 3-hydroxyflavanone and then followed by further oxidation into 3-hydroxyflavone. If an OMe′ or methyl substituent is present in the 6′-position of the chalcone, aurones rather than 3-hydroxyflavones are obtained and the reaction is affected at room temperature. Various theories have been presented as to why cyclisation of a chalcone epoxide intermediate takes place by attack of the phenolic oxygen group at the α-position rather than at the β-position. One such theory is that displacement of the carbonyl group out of the plane of the phenolic ring by steric interaction with the 6′-methoxy or methyl group increases the distance of phenolic oxygen from the β-position more than from that of the α-position. Another is that the previously mentioned steric interaction favors the product with the smaller heterocyclic ring. Dean and Podimuang suggested that such effects are not large and at temperatures of more than 20 °C, they diminish rapidly and pyrone derivatives are again the main products.

To reinvestigate this ambiguity of mechanism at the molecular level, we consider a quantum chemical calculation taking 2′-hydroxychalcone as the model compound rather than its 6-substituted derivative. Four reaction pathways, A–D, have been considered in Schemes 1–4. We adopt the DFT approach, but the selection of functional and basis sets becomes bizarre due to the hundreds of newly proposed DFT functionals and basis sets. Godmann and Simon[12] recently revealed that compared with the newly developed meta GGA, meta-hybrid GGA and functional, old B3LYP are still good choices for optimizing transition states and hence appropriate for studying organic reaction mechanisms. Consistent with recent quantum chemical study of chalcones[13] and flavonoids,[14] we consider 6-31+G(d,p) atomic basis as a good choice for our present calculation.

Computational details

We adopt the density functional theory (DFT) method of Becke's three-parameter exchange and gradient-corrected correlation functional of Lee, Yang and Parr (B3LYP[15]) for optimization of the reactants, transition states, intermediates, and products. A double-zeta quality GTO (Gaussian-type orbital) atomic basis function augmented by diffuse function on heavy atoms, 6-31+G(d,p) has been widely used in the present investigation. Vibrational analysis has been carried out at stationary points under harmonic approximation to check the optimized geometry of reactant, intermediate, and product characterized by all real frequency and transition states (TS), characterized by only one imaginary frequency. All transition states have been confirmed by the presence of one imaginary frequency, and the reactant, intermediate, and product are confirmed as stationary points by the presence of all real frequencies. Each TS has been confirmed by the intrinsic reaction coordinate (IRC) calculation by the connectivity of the corresponding intermediates in the respective potential energy surface. To account for the solvent effect, all optimization with the polarizable continuum model (PCM) was carried out at the B3LYP/6-31+G(d,p) level with ethanol as the solvent since this solvent was used in the experimental study. Apart from the wide applicability and reliability of the B3LYP functional predicting activation energy in the theoretical investigation of the organic chemistry reaction mechanism, we used some recently developed DFT functionals, particularly WB97XD,[16] CAM-B3LYP,[17] M06-2X,[18] BMK,[19] and HCTH/407,[20] which have proven useful and gained acceptance in recent years, for single-point calculation of the reactants, intermediates, transition states, and products. However, the solvation effect has been considered only in the B3LYP method. It should be noted that optimization has been carried only in the B3LYP level due to its good reputation in reproducing

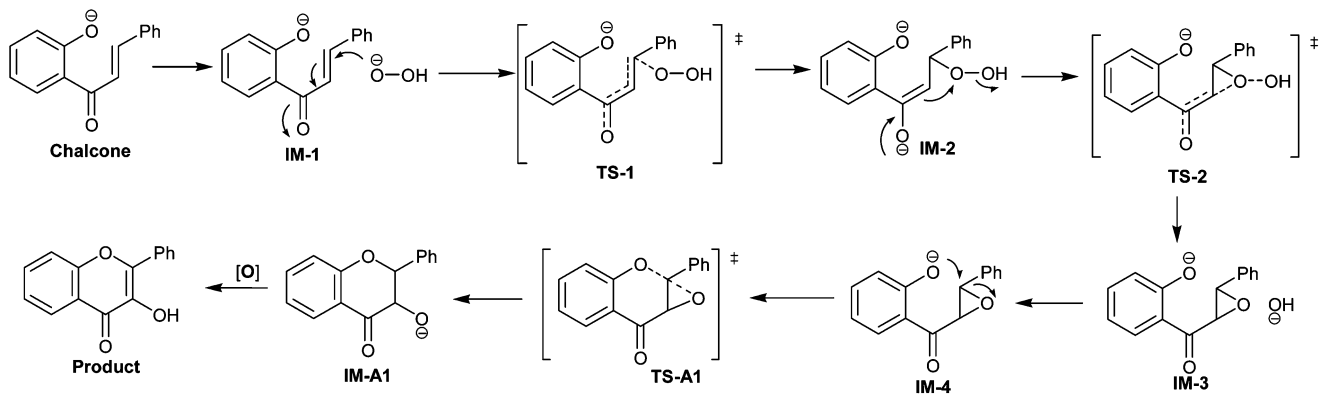

Scheme 1

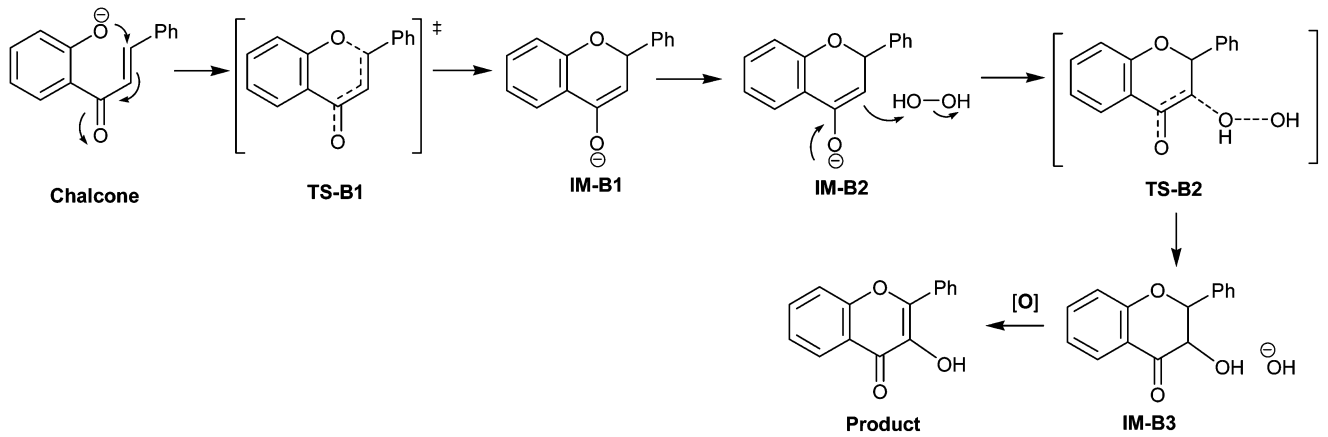

Scheme 2

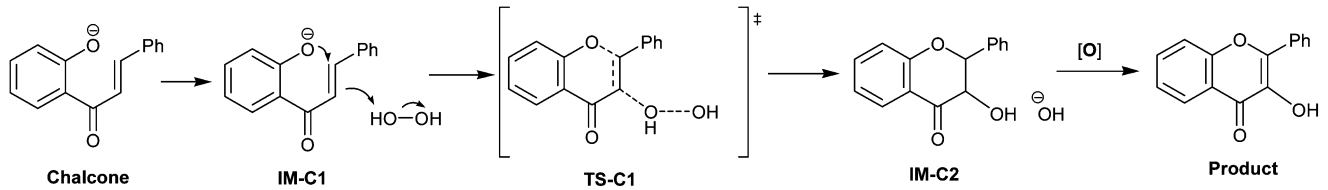

Scheme 3

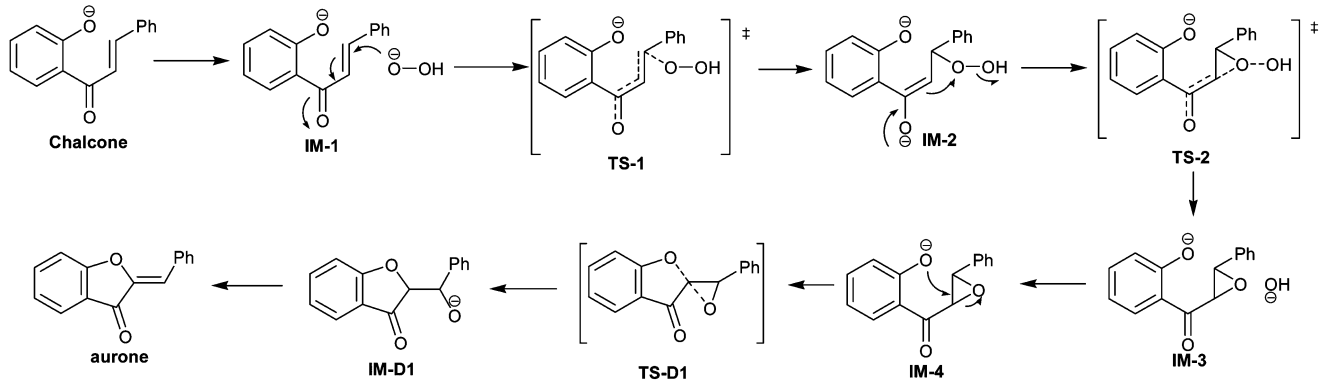

Scheme 4

geometries. Gibb's free energy (G) has been evaluated at 298 K and 1 atm pressure. All computation has been carried out by the G09[21] quantum chemistry package.

Results and discussions

We formulated four different theoretical reaction pathways for the formation of flavanones from chalcones. Path-A consists of 1,4 Michael addition of peroxide ions to chalcones *via* formation of an epoxide intermediate **IM-4**. In the next step, further ring opening of **IM-4** at the β-position leads to product. Whereas in path-B initial cyclization of chalcones leads to **IM-B1**, further hydroxylation by hydrogen peroxide yields the final product. In the case of path-C, simultaneous cyclization and hydroxylation occurred leading to product, but path-D is similar to path-A in the first six steps. The ring opening of **IM-4** at the α-position leading to path-D, and the product finally gave aurone rather than flavones.

(1) Epoxidation *via* Michael addition followed by six-member TS (path-A) ring opening.

(2) Enolization by self cyclization, followed by hydroxylation (path-B).

(3) Simultaneous cyclization and hydroxylation (path-C).

(4) Epoxidation *via* Michael addition followed by five-member TS (path-D) ring opening of epoxide.

Relative Gibbs free energy (gas phase and in ethanol) of the considered intermediates, transition states, and products have been given in Tables 1–4, respectively, for each associated

Table 1 Relative Gibbs free energy of the intermediates and transition states of path-A in different DFT functionals at 6-31+G(d,p)[a]

	B3LYP	WB97XD	CAM-B3LYP	BMK	M06-2X	HCTH/407
Reactant	0.00	0.00	0.00	0.00	0.00	0.00
IM-1	56.73 (10.91)	55.40	58.14	57.83	55.03	51.34
TS-1	60.49 (28.79)	58.13	61.22	61.14	56.62	56.01
IM-2	54.11 (14.28)	49.92	53.56	49.95	46.39	49.71
TS-2	54.42 (24.08)	51.58	55.13	51.22	48.93	48.27
IM-3	25.21 (−13.52)	15.83	19.61	14.49	11.83	19.41
IM-4	−34.05 (−39.67)	−41.08	−38.36	−41.87	−42.53	−39.53
TS-A1	10.36 (−1.12)	9.89	12.64	6.46	12.83	2.48
IM-A1	−26.29 (−39.83)	−36.89	−33.06	−39.51	−37.76	−27.03
Product	−59.47 (−108.00)	−65.68	−64.54	−67.19	−62.93	−61.18

[a] Relative Gibb's free energy in ethanol has been given in brackets.

Table 2 Relative Gibbs free energy of the intermediate and transition state of path-B in different DFT functionals at 6-31+G(d,p)[a]

	B3LYP	WB97XD	CAM-B3LYP	BMK	M06-2X	HCTH/407
Reactant	0.0	0.00	0.00	0.00	0.00	0.00
TS-B1	17.91 (17.62)	15.50	16.25	15.84	14.87	16.11
IM-B1	13.28 (11.84)	6.73	8.46	8.10	4.94	13.63
IM-B2	3.02 (8.43)	−4.21	−3.18	−1.40	−7.08	6.68
TS-B2	20.09 (24.91)	20.03	20.09	21.82	20.97	18.01
IM-B3	−52.13 (−52.40)	−62.43	−60.94	−63.94	−65.24	−48.35
Product	−92.77 (−129.33)	−97.70	−97.79	−101.57	−97.30	−91.66

[a] Relative Gibb's free energy in ethanol has been given in brackets.

Table 3 Relative Gibbs free energy of the intermediate and transition state of path-C in different DFT functionals at 6-31+G(d,p)[a]

	B3LYP	WB97XD	CAM-B3LYP	BMK	M06-2X	HCTH/407
Reactant	0.00	0.00	0.00	0.00	0.00	0.00
IM-C1	−4.44 (1.96)	−3.68	−3.62	−0.56	−3.87	−2.30
TS-C1	10.95 (18.21)	7.71	8.91	11.11	7.25	11.71
IM-C2	−4.42 (2.07)	−3.69	−3.62	−0.59	−3.89	−2.29
Product	−92.77 (−129.33)	−97.70	−97.79	−101.57	−97.30	−91.66

[a] Relative Gibb's free energy in ethanol has been given in brackets.

reaction path. To compare solvation dependency of the calculate activation energy parameter, all structures were optimized in ethanol (PCM model) at the B3LYP/6-31+G(d,p) level of theory. In addition, all optimized structures of intermediates are given in Fig. 1. All transition states, reactants, and products are given in Fig. 2. We have arranged the article in four sections to discuss the mechanism for each step.

Table 4 Relative Gibbs free energy of the intermediate and transition states of path-D in different DFT functionals at 6-31+G(d,p)[a]

	B3LYP	WB97XD	CAM-B3LYP	BMK	M06-2X	HCTH/407
Reactant	0.00	0.00	0.00	0.00	0.00	0.00
IM-1	56.72 (10.91)	55.40	58.41	57.83	55.03	51.34
TS-1	60.49 (28.79)	58.13	61.22	61.14	56.62	56.01
IM-2	54.11 (14.28)	49.92	53.56	49.95	46.39	49.71
TS-2	54.42 (24.08)	51.58	55.13	51.22	48.93	48.27
IM-3	25.21 (−13.52)	15.83	19.61	14.49	11.83	19.41
IM-4	−34.06 (−39.67)	−41.08	−38.36	−41.87	−42.53	−39.53
TS-D1	−14.24 (−20.12)	−18.57	−15.97	−19.27	−15.82	−19.81
IM-D1	−26.35 (−38.21)	−35.98	−31.37	−36.68	−35.23	−31.32
Product	−4.20 (−46.87)	−6.27	−6.59	−6.69	−2.43	−7.95

[a] Relative Gibb's free energy in ethanol has been given in brackets.

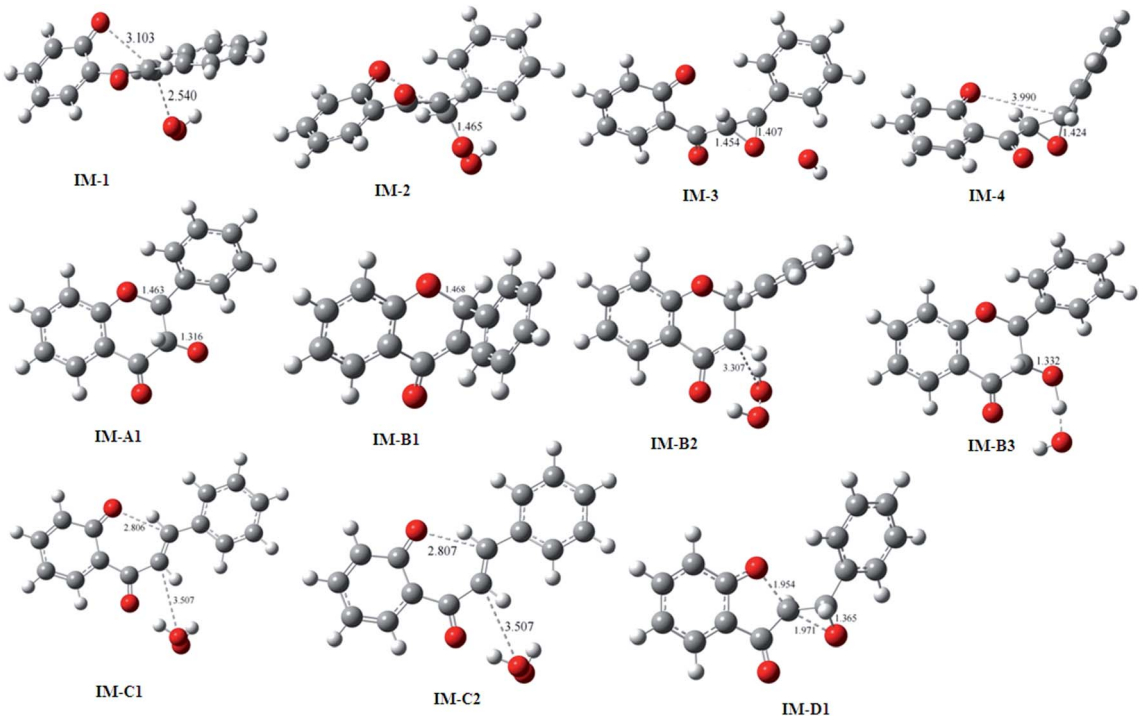

Fig. 1 Optimized structures of all the intermediates.

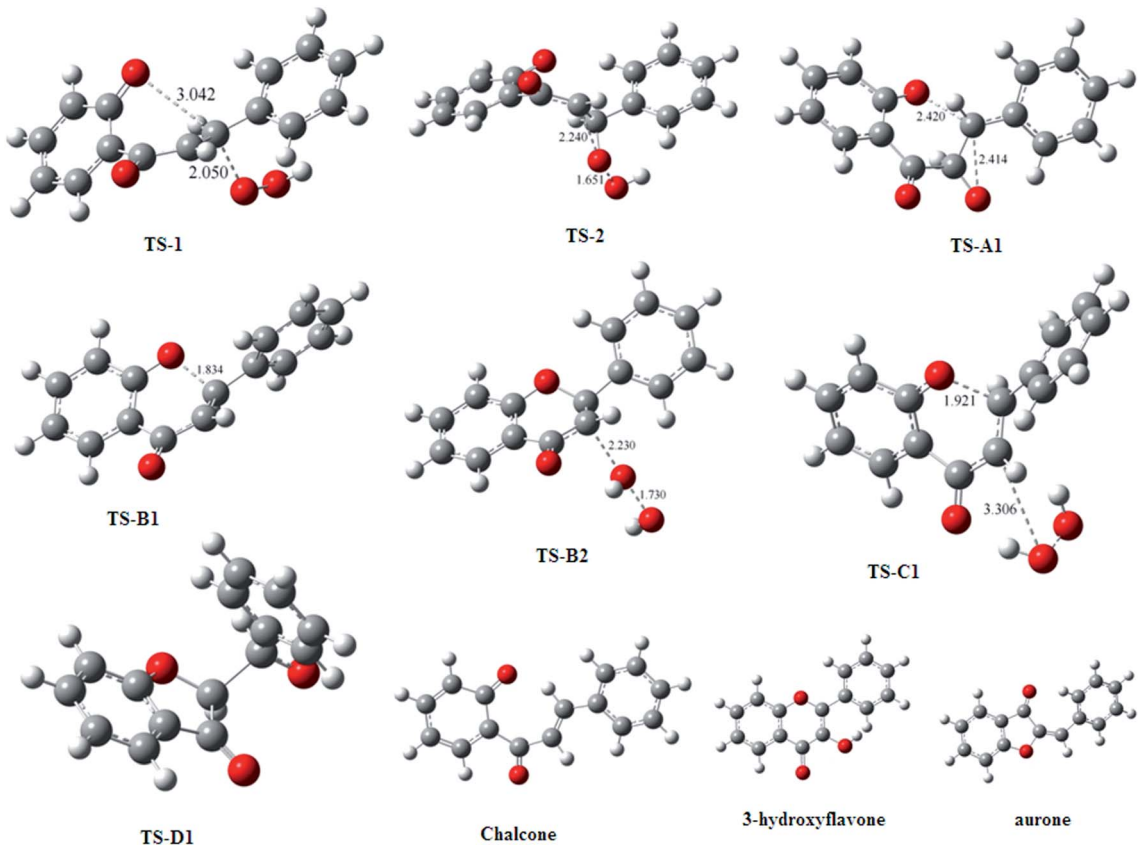

Fig. 2 Optimized structures of all the transition states, reactants, and products.

Path-A involves the Michael addition of the peroxide ion (Scheme 1) to the conjugated C_α=C_β double bond of chalcone, which requires formation of a pre-reactive intermediate **IM-1**, where the peroxide ion interaction from a distance of 2.54 Å causes a slight elongation (0.01 Å) of the conjugated C_α=C_β distance than the ground state of chalcone.

It should be noted that **IM-1** energy remains very high by 56.73 kcal mol^{-1} in B3LYP. In addition, due to higher solvation, the energy value in ethanol was decreased to 10.9 kcal mol^{-1}. The predicted transition state (**TS-1**) was found to be just 3.76 kcal mol^{-1} higher relative to **IM-1**, with a shortening of C_β–O distance (2.050 Å) and an elongation of C_α=C_β distance (1.850 Å). However, in ethanol, $\Delta G^{\#}$ was increased to 17.88 kcal mol^{-1} due to greater solvation of **IM-1** compared with **TS-1**. It is because the dissipation of the negative charge in **TS-1** becomes less solvated. Estimated activation energy ($\Delta G^{\#}$) in various DFT functionals is highly consistent, ~4–5 kcal mol^{-1}. The intermediate **IM-2** having C_β–O distance of 1.455 Å predicted the β hydroperoxide formation. This unstable intermediate readily underwent rapid epoxidation with a very small activation barrier height of 0.31 kcal mol^{-1} (B3LYP) relative to **IM-2**, to the unstable intermediate IM3, which subsequently forms the more stable **IM-4** (−34.05 kcal mol^{-1} in B3LYP). The calculated $C_{\alpha/\beta}$–O bond distances (1.44 Å and 1.42 Å) of epoxide **IM-4** are not equal. The ring opening of epoxide **IM-4** occurred by the attack of phenolic oxygen at C_β of the epoxide. The calculated gas phase activation energy $\Delta G^{\#}$ (44.41 kcal mol^{-1}) was very large and unlikely to be achieved at room temperature. This large gas phase activation barrier can be attributed from the reorganization of proper **IM-4** conformation for bonding interaction due to a larger C_β–O bond (3.990 Å) distance. However, in ethanol activation energy, $\Delta G^{\#}$ of the ring opening of epoxide **IM-4** remained in higher order (38.55 kcal mol^{-1}). This fact suggests that solvation has negligible effect on the ring opening of epoxide **IM-4** by an attack of phenolic oxygen at C_β of the epoxide. Aromatisation of **IM-A1** leads to the desired product 3-hydroxyflavone. From the TS diagram of path-A in (Fig. 3) it can be seen that the pre-reactive complex formation is energetically unfavourable (56.73 kcal mol^{-1}) in the gas phase as well as in solvent phase (10.91 kcal mol^{-1}) and unlikely to be proceed further unless under high temperatures.

Path-B predicted the initial cyclization (Scheme 2) of chalcone by the nucleophilic attack of phenolic oxygen at conjugated C_α=C_β that pass through an activation barrier ($\Delta G^{\#}$) of 17.91 kcal mol^{-1} (in gas phase B3LYP), which is not affected in ethanol (17.62 kcal mol^{-1}), to produce the enol intermediate **IM-B1**. The gas phase calculated $\Delta G^{\#}$ value has been found to be consistent in WB97XD, CAM-B3LYP, BMK, and HCTH/407 with the exception of M06-2X and B3LYP, where it has been slightly lowered and overshot, respectively. Associated shortening of the C_β–O bond by ~35%, with respect to C_β–O distance of ground state of chalcone would be worthy of mention. The formation of an α hydroperoxide requires an interaction of **IM-B1** with H_2O_2, which stabilizes the intermediate **IM-B2** by ~11 kcal mol^{-1} in various DFT functionals. This small energy stabilization of **IM-B2** can be envisaged from the weak interaction of H_2O_2, which has a C–O bond distance of 3.307 Å from the α carbon of the enol. α-Hydroxylation of the cyclic intermediate **IM-B2**. This is initiated by the significant negative charge of the α-carbon atom (−0.407 a.u), which passes through the transition state (**TS-B2**)

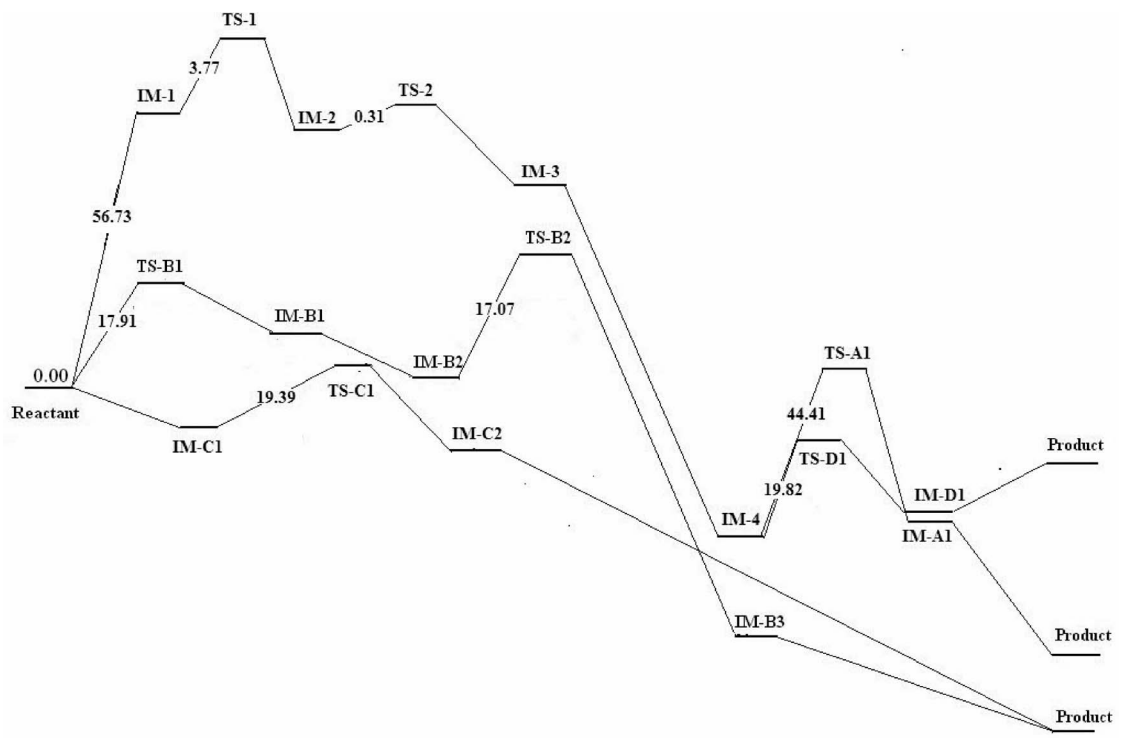

Fig. 3 Potential energy surface (gas phase) and Gibbs free energy of activation (kcal mol^{-1}) at B3LYP/6-31+G(d,p).

having an activation energy barrier 17.07 kcal mol^{-1} (gas phase) and is almost unaffected in ethanol (17.48 kcal mol^{-1}). The C_α–O bond distance has been significantly reduced by 33% with respect to **IM-B2** during the course of the reaction. The predicted activation energy barrier ($\Delta G^{\#}$), relative to **IM-B2** in various DFT functionals, is not consistent but rather bizarre. The hydroxylated intermediate **IM-B3**, having the C_α–O distance 1.316 Å signifying the existence of the C–OH bond, has been found to be very stable (~60 kcal mol^{-1} with respect to the reactant) and rapidly aromatized to the more stable 3-hydroxyflavone. The calculated stability of 3-hydroxyflavone has been found consistent in the selected DFT functional. It is interesting to note that solvation does not change the activation energy parameters significantly.

In contrast, path-C predicts the cyclization (Fig. 3) of chalcone with simultaneous hydroxylation, which requires a proper interaction for bonding conformation (**IM-C1**) of chalcone with H_2O_2. The predicted very low interaction energy (~3 kcal mol^{-1} in various DFT functional) of **IM-C1** could be ascertained from negligible shortening of the C_β–O distance (0.52%) and weak interaction arising from longer (3.507 Å) C_α–O of H_2O_2 interaction. This weakly bound intermediate **IM-C1** passed through the transition state (**TS-C1**) with the formation of C_α–O (1.912 Å) and C_β–O (3.213 Å) bonds, which are significantly shorter than the precursor intermediate **IM-C1**. The associated gas phase calculated $\Delta G^{\#}$ relative to **IM-C1** has been found to be quite small, estimated as ~11–14 kcal mol^{-1} by B3LYP, BMK, and HCTH/407 and ~8 kcal mol^{-1} in WB97XD and CAM-B3LYP. Interestingly, B3LYP-estimated $\Delta G^{\#}$ in ethanol has been found 16.25 kcal mol^{-1}, which is slightly higher arising from poor solvation of **TS-C1**. Thus instead of the initial enolization of chalcone (path-B), simultaneous cyclization and hydroxylation (path-C) would be an energetically more suitable choice, but the marginal difference in $\Delta G^{\#}$ (~4 kcal mol^{-1}) values could not establish path-C as a major choice over path-B even at room temperature. It should be noted that hydroxylated intermediate **IM-C2** is quite stable (−4.42 kcal mol^{-1} in B3LYP) and readily aromatized to more (−92.77 kcal mol^{-1} in B3LYP) stable 3-hydroxyflavone.

Path-D is similar to path-A, up to the formation of epoxide **IM-4**. Apart from path-A, the epoxide ring (Fig. 3) opening has been considered by the attack of phenolic oxygen at α carbon with a distance of 2.820 Å. An ~31% shortening of O–C_α has been occurred in **TS-D1** formation. The gas phase estimated activation energy barrier ($\Delta G^{\#}$) of the five-member transition state (**TS-D1**) is relatively small (~19.82 kcal mol^{-1}) compared with that of the six-member transition state (**TS-A1**) in path-A (44.41 kcal mol^{-1}), as estimated by B3LYP. Although the activation energy $\Delta G^{\#}$ of the five-member transition state (**TS-D1**) is unaffected (19.55 kcal mol^{-1}) in ethanol, but it still remains lower than that of the $\Delta G^{\#}$ of six-member transition state **TS-A1** (38.55 kcal mol^{-1}) by a significant margin. Due to this low activation energy barrier, the epoxide opening occurs *via* the five-member transition state **TS-D1** to give aurone rather than 3-hydroxyflavone. It is noteworthy that the fused five-member ring intermediate **IM-D1** has been found to be slightly more stable than **IM-A1** by 0.06 kcal mol^{-1} in B3LYP. In addition, it is important to note that final aurone product is thermodynamically less stable than 3-hydroxyflavone in the gas phase, as well as in ethanol.

Conclusion

The present computational investigation based on B3LYP/6-31+G(d,p) optimization reveals the mechanistic diversity of the Algar–Flynn–Oyamada (AFO) reaction. Four possible mechanistic paths have been considered, which involve hydroxylation of chalcones either by the conventional addition–hydroxylation reaction or epoxidation followed by ring opening of epoxide, mediated by alkaline hydrogen peroxide through different TS, which leads to different final products. Our calculations support previous proposals of Dean and co-workers, that epoxidation is unlikely to occur due to electrostatic interaction of the peroxide anion with the conjugated C=C double bond. Although $\Delta G^{\#}$ of **TS-1**, relative to **IM-1**, is negligible, the interaction energy of **IM-1** is considerably higher (56.73 kcal mol^{-1}) and unlikely to form at room temperature. Thus, only at high temperatures would **IM-1** be formed and the resulting epoxide produced finally lead to aurone as the major product by following path-D due to the lower $\Delta G^{\#}$ of the five-member transition state (**TS-D1**), compared with that of the six-member transition state (**TS-A1**) of path-A epoxide ring opening. From the current study, we also concluded that under the solvent model, the free energy barrier of path-A/D is ~11 kcal mol^{-1}, which is possible to overcome by introducing the substituent effect. Thus, under solvation model studies also suggested that if the 6′ position of chalcone is occupied by a group like OMe or methyl, simultaneously, path-D can also be possible. However, due to the negligible difference in $\Delta G^{\#}$ value of hydroxylation of enol and simultaneous attack, path-B and path-C are equally probable even at room temperature. The inclusion of the solvation effect on activation energy also supports the gas phase conclusion. DFT functionals currently used to predict consistency with $\Delta G^{\#}$ although they have different total energy due to different XC (exchange–correlation) sections.

References

1 (*a*) T. A. Geissman, in *Modern Methods of Plant Analysis*, ed. K. Paech and M. V. Tracey, Springer, Berlin, Heidelberg, 1955, vol. 3, p. 450; (*b*) K. E. Schwinn and K. M. Davies, in *Annual Plant Reviews: Plant Pigments and their Manipulation*, ed. K. M. Davies, 2009, vol. 14, p. 92.

2 (*a*) K. S. Krogholm, Ph.D. thesis, Department of Human Nutrition, Faculty of Life Sciences, University of Copenhagen, 2011; (*b*) E. C. Bate-Smith, *Adv. Food Res.*, 1954, **5**, 261; (*c*) H. M. Merken and G. R. Beecher, *J. Agric. Food Chem.*, 2000, **48**, 577; (*d*) F. P. Gonord, L. P. R. Bidel, A. L. Fanciullino, H. Gautier, F. L. Lopez and L. Urban, *J. Agric. Food Chem.*, 2010, **58**, 12065.

3 (*a*) P. G. Pietta, *J. Nat. Prod.*, 2000, **63**, 1035; (*b*) A. S. Saraf and E. T. Oganesyan, *Pharm. Chem. J.*, 1991, **25**, 65; (*c*) L. Pistelli and I. Giorgi, *Dietary Phytochemicals and Microbes*, 2012, vol. 33; (*d*) R. M. De Conti Lourenço, P. Da Silva Melo and

A. B. Albino de Almeida, *Antifungal Metabolites from Plants-II*, ed. M. R. Abyaneh and M. Rai, Springer, Berlin, Heidelberg, 2013, p. 283; (*e*) T. N. Kaul, E. Middleton and P. L. Ogra, *J. Med. Virol.*, 1985, **15**, 71; (*f*) P. Batra and A. K. Sharma, *3 Biotech.*, 2013, **3**, 439; (*g*) W. Ren, Z. Qiao, H. Wang, L. Zhu and L. Zhang, *Med. Res. Rev.*, 2003, **23**, 519; (*h*) M. K. Chahar, N. Sharma, M. P. Dobhal and Y. C. Joshi, *Pharmacogn. Rev.*, 2011, **5**, 1.

4 A. Crozier, I. B. Jaganath and M. N. Clifford, *Plant Secondary Metabolites: Occurrence, Structure and Role in Human Diet*, ed. A. Crozier, M. N. Clifford and H. Ashihara, Blackwell Publishing Ltd., 2006, p. 1.

5 (*a*) E. Middleton Jr, C. Kandaswami and T. C. Theoharidas, *Pharmacol. Rev.*, 2000, **52**, 673; (*b*) A. D. Agrawal, *Int. J. Pharm. Sci. Nanotechnol.*, 2011, **4**, 1394; (*c*) T. Shohaib, M. Shafique, N. Dhanya and M. C. Divakar, *Hygeia: J. Drugs Med.*, 2011, **3**, 1.

6 (*a*) Z. P. Xiao, Z. Y. Peng, M. J. Peng, W. B. Yan, Y. Z. Ouyang and H. L. Zhu, *Mini-Rev. Med. Chem.*, 2011, **11**, 169; (*b*) L. H. Yao, Y. M. Jiang, J. Shi, F. A. Tomás-Barberán, N. Datta, R. Singanusong and S. S. Chen, *Plant Foods Hum. Nutr.*, 2004, **59**, 113; (*c*) J. Kühnau, *World Rev. Nutr. Diet.*, 1976, **24**, 117.

7 (*a*) S. Gunduz, A. C. Goren and T. Ozturk, *Org. Lett.*, 2012, **14**, 1576; (*b*) T. H. Minton and H. Stephen, *J. Chem. Soc.*, 1922, **122**, 1598; (*c*) B. H. Ingham, H. Stephen and R. Timpe, *J. Chem. Soc.*, 1931, 895; (*d*) H. F. Dean and M. Nierenstein, *J. Am. Chem. Soc.*, 1925, **47**, 1676.

8 (*a*) T. Oyamada, *J. Chem. Soc. Jpn.*, 1934, **55**, 1256; (*b*) J. Algar and J. P. Flynn, *Proc. R. Ir. Acad., Sect. B*, 1934, **42B**, 1; (*c*) J. J. Li, *Name Reactions*, Springer, Berlin, Heidelberg, 2009, vol. 6.

9 (*a*) T. R. Gormley and W. I. O'Sullivan, *Tetrahedron*, 1973, **29**, 373.

10 F. M. Dean and V. Podimuang, *J. Chem. Soc.*, 1965, 3978.

11 (*a*) D. M. Fitzgerald, J. F. O'Sullivian, E. M. Philbin and T. S. Wheeler, *J. Chem. Soc.*, 1955, 860–862; (*b*) T. R. Gormley and W. I. O'Sullivan, *Tetrahedron*, 1973, **29**, 369–373.

12 L. Simon and J. M. Godmann, *Org. Biomol. Chem.*, 2011, **9**, 689.

13 Y. Xue, L. Zhang, Y. Li, D. Yu, Y. Zheng, L. An, X. Gong and Y. Liu, *J. Phys. Org. Chem.*, 2013, **26**, 240–248.

14 D. Zhang, Y. Liu, L. Chu, D. Wang, S. Cai, F. Zhou and B. Ji, *J. Phys. Chem. A*, 2013, **117**, 1784–1794.

15 (*a*) A. D. Becke, *J. Chem. Phys.*, 1993, **98**, 1372–1377; (*b*) A. D. Becke, *J. Chem. Phys.*, 1993, **98**, 5648–5652.

16 J. D. Chai and M. Gordon, *Phys. Chem. Chem. Phys.*, 2008, **10**, 6615–6620.

17 T. Yanai, D. Tew and N. Handy, *Chem. Phys. Lett.*, 2004, **393**, 5157.

18 Y. Zhao and D. G. Truhlar, *J. Chem. Phys.*, 2006, **125**, 194101.

19 A. D. Boese and M. L. Martin, *Chem. Phys.*, 2004, **121**, 3405–3416.

20 A. D. Boese and N. C. Handy, *J. Chem. Phys.*, 2001, **114**, 5497–5503.

21 M. J. Frisch, G. W. Trucks, H. B. Schlegel, G. E. Scuseria, M. A. Robb, J. R. Cheeseman, G. Scalmani, V. Barone, B. Mennucci and G. A. Petersson, *et al.*, *Gaussian 09, Revision A.02*, Gaussian, Inc., Wallingford, CT, 2009.